Direct Functionalization of Polysaccharide-Based Xylan Phenyl Carbonate Nanoparticles with Tumor Cell Specific Antibodies

Bilemjian, Vrouyr; Lin, Yusheng; Wan, Wei; Egri, Gabriella; Huls, Gerwin; Heinze, Thomas; Bremer, Edwin; Gericke, Martin; Dähne, Lars

Published in:
ChemBioChem

DOI:
10.1002/cbic.202300828

Publication date:
2024

ChemBioChem

Research Article
doi.org/10.1002/cbic.202300828

Chemistry Europe
European Chemical Societies Publishing

www.chembiochem.org

Direct Functionalization of Polysaccharide-Based Xylan Phenyl Carbonate Nanoparticles with Tumor Cell Specific Antibodies

Vrouyr Bilemjian,[a, b] Yusheng Lin,[b] Wei Wan,[a] Gabriella Egri,[a] Gerwin Huls,[b] Thomas Heinze,[c] Edwin Bremer,[b] Martin Gericke,*[c] and Lars Dähne*[a]

An efficient and easy-to-use approach is presented for obtaining biocompatible polysaccharide-based nanoparticles (NP) that can act as tumor-specific drug delivery agents. Two antibodies are directly immobilized onto reactive xylan phenyl carbonate (XPC) NP; namely Cetuximab (CTX) that binds to human epidermal growth factor receptor (EGFR) and Atezolizumab (ATZ) that binds to programmed death-ligand 1 (PD-L1). High coupling efficiency (up to 100 %) are achieved without any pre-activation and no aggregation occurs during antibody immobilization. By quartz crystal microbalance experiments with dissipation monitoring (QCM-D), flow cytometry assays, and confocal laser scanning microscopy imaging it is demonstrated that the functionalized XPC-NP specifically bind to cells carrying the corresponding antigens. Moreover, the NP retain the antibody specific bioactivities (growth inhibition for CTX and induction of T-cell cytotoxicity for ATZ).

Introduction

As the second-leading cause of mortality, cancer is one of the major public health issues facing the world today.[1] Surgery, radiation therapy, chemotherapy, targeted therapy, and hormone therapy are some of the traditional therapeutic modalities utilized in the treatment of cancer.[2] Despite their capacity for immunomodulation and cytotoxicity, radiation and chemotherapy is frequently associated with severe side effects and a substantial risk of recurrences.[3] Recent advances in nanotechnology have produced novel chemical, physical, and biological features in nanoscale materials. In particular, the application of nanotechnology is applied in the delivery of drugs. Since nanoparticles (NP) can be an effective drug delivery technique, nanotechnology has been intensively researched and used to treat cancer.[4]

Nanoparticle-based drug administration has distinct benefits over conventional drug delivery methods, including greater stability and biocompatibility, especially in challenging environments. Moreover, it can increase permeability and absorption while allowing for fine-tuning and targeted delivery to specific cells or tissues, thereby bolstering drug efficacy and minimizing off-target effects.[1,5] Additionally, researchers have lately begun to look into how immunotherapy, which is increasingly crucial in the treatment of cancer, uses NP.[5e,6] Doxil® (doxorubicin, enunciated in liposomes, approved by the United State Food and Drug Administration (FDA) in 1995) and Abraxane® (paclitaxel, enunciated in albumin NP, approved by FDA in 2006) are two of the most prominent antitumor nanotherapeutics that have been identified by using the passive mechanisms of enhanced permeability and retention (EPR). Both of these antitumor nanomedicine compositions have been approved by the FDA.[7] Up to now FDA has not given its approval for any active targeting of malignancies through receptor-mediated targeting employing formulations based on NP. The integration of cancer-specific antibodies, particularly those that are already defined in clinics, such as anti-human EGFR (epidermal growth factor receptor) or anti-PD-L1 (anti-programmed death ligand 1), with novel NP-based drug-delivery vectors is one possibility for overcoming the current lack of clinical translation.

Although current cancer immunotherapies have revolutionized cancer treatment, their non-specific immune response can lead to severe side effects. To develop safer and more effective cancer immunotherapy, researchers are exploring innovative approaches, including NP-based drug delivery systems. These systems can harness the immune system's power in a targeted and precise manner, representing a significant advancement in cancer treatment. Polysaccharides-based NP are of particular interest due to their simplicity in manufacture, preferred biocompatibility, and most importantly effectiveness in modifying immune responses.[8] In order to alter the immune system's chemotactic factor and cytokine-releasing status, maintain the balance among T helper (Th) type 1 and 2 cell, restrict the

[a] V. Bilemjian, W. Wan, G. Egri, L. Dähne
Surflay Nanotec GmbH, 12489 Berlin, Germany
E-mail: l.daehne@surflay.com

[b] V. Bilemjian, Y. Lin, G. Huls, E. Bremer
Department of Hematology, University Medical Center Groningen, University of Groningen, 9713 GZ Groningen, The Netherlands

[c] T. Heinze, M. Gericke
Friedrich Schiller University Jena, Institute of Organic Chemistry and Macromolecular Chemistry, Center of Excellence for Polysaccharide Research, 07743 Jena, Germany
E-mail: martin.gericke@uni-jena.de

Supporting information for this article is available on the WWW under https://doi.org/10.1002/cbic.202300828

representation of matrix metalloproteinase, and prevent the growth of tumor vessels, polysaccharides have been found to be effective.[9] Additionally, recent research has shown that polysaccharides, particularly botanical polysaccharides, can effectively stimulate macrophage proliferation and support their phagocytic activity toward foreign objects and tumor cells.[9a,10]

Polysaccharide-based NP provide inherent advantages in the context of biomedical applications due to their inherent biocompatibility and potential biodegradability.[11] Moreover, they are easily accessible by self-assembling of hydrophobically modified polysaccharide derivatives.[12] These types of polysaccharide-based NP are taken up by cells, which makes them very attractive for drug delivery applications.[13] A key challenge for the development of novel nanomaterials in this context is the functionalization of polysaccharide NP. Of particular interest are antibodies that enable cell type specific targeting. Considering that these biomolecules are rather expensive and sensitive, the functionalization procedures should (i) be efficient and with high conversion yields, (ii) work under mild aqueous reaction conditions, and (iii) should avoid laborious activation steps and aim to minimize the number of process and purification steps to avoid loss of the valuable functional nanomaterials and reduce costs and time requirements. Recently, NP derived from xylan phenyl carbonates (XPC) have been reported that are easy to prepare and can be coupled directly with dyes carrying amino groups within one step at high conversion rates.[14] It is hypothesized that these reactive XPC-NP can be functionalized directly with tumor targeting antibodies without the need for any preactivation and that the materials obtained can be used for tumor cell specific drug delivery (Figure 1).

Although the EPR mechanism makes it easier for therapeutic cargo to accumulate in tumor tissue, it does not guarantee that the cargo will be delivered to tumor cells. The cellular internalization of nanovesicles that are accumulated by the EPR mechanism is dependent on a spatio-temporal membrane-mediated mechanism.[15] These activities might not happen in a controlled and regular manner and, over the course of time, there might be a build-up of vehicles inside the tumor stroma, which would result in a reverse gradient of vehicular permeation. Given such options, researchers have investigated the possibility of integrating additional processes within the nano vehicles to facilitate the internalization of tumor cells or to target the tumor immune microenvironment.[7a] Therefore, our research has been designed with the purpose of conjugating cancer cell targeting antibodies Cetuximab (CTX) and Atezolizumab (ATZ) onto the surface of XPC-NP and directing those to the cancer cells or the tumor microenvironment as active targeting and site-specific delivery of those NP. Combining such antibodies, which are already used in clinical settings, with a novel NP in order to achieve site-specific delivery would present exciting opportunities for the creation of novel site-specific XPC-NPs.

Results and Discussion

Preparation and Dye-Labeling of Xylan Phenyl Carbonate Nanoparticles

Polysaccharide-based nanoparticles (NP) were prepared as previously described.[14a] In short, hydrophilic xylan phenyl carbonate (XPC) was synthesized by chemical derivatization of the polysaccharide xylan with phenyl chloroformate under homogeneous reaction conditions. XPC-NP were obtained by a facile dialysis of a solution of XPC in *N*,*N*-dimethyl acetamide (DMA) against water. Upon the slow exchange of the solvent (DMA) against the non-solvent (water), self-assembling of XPC into spherical NP occurred. Using this process, aqueous particle dispersions with particle sizes of about 250 nm were obtained and used in this study (Figure 2). In addition, dye-labeled XPC-NP were of interest in order to later visualize the tumor cell targeting upon antibody conjugation. It has been demonstrated previously that XPC-NP are reactive towards compounds with amino moieties, which enabled direct immobilization of dyes on the particle surface subsequent to NP preparation by the dialysis approach.[14b] However, this could potentially block some of the reactive PC moieties that are required for the later immobilization of antibodies. Thus, an alternative approach for *in situ* dye labeling prior to the actual XPC-NP preparation through dialysis induced self-assembling was studied. XPC was dissolved in DMA (4.5 mg/ml) and converted with a small amount of sulforhodamine amine (0.01 equivalents per PC moiety) under homogeneous conditions according to the procedures employed for the synthesis of xylan carbamates from XPC.[16] The resulting product, a XPC derivative were a small amount of carbonate moieties ($\leq$1%) were replaces by

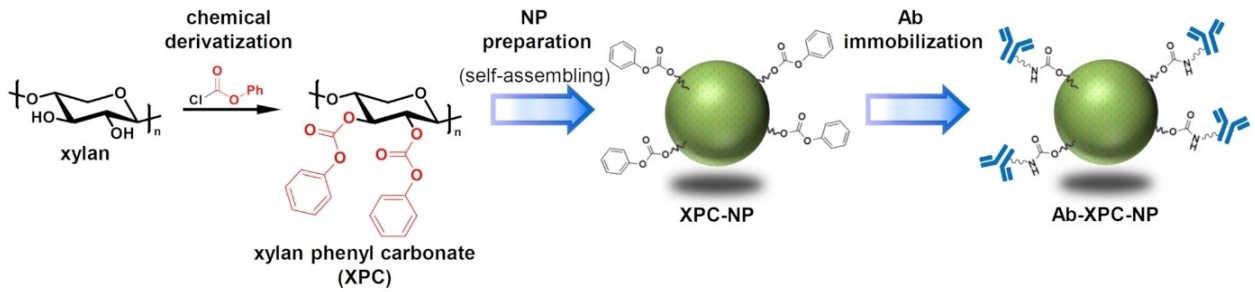

Figure 1. Schematic representation of the chemical conversion of xylan into xylan phenyl carbonate (XPC), the formation of XPC nanoparticles (NP) by self-assembling, and the subsequent immobilization of the tumor-targeting antibodies (Ab) Cetuximab and Atezolizumab on the surface of XPC-NP.

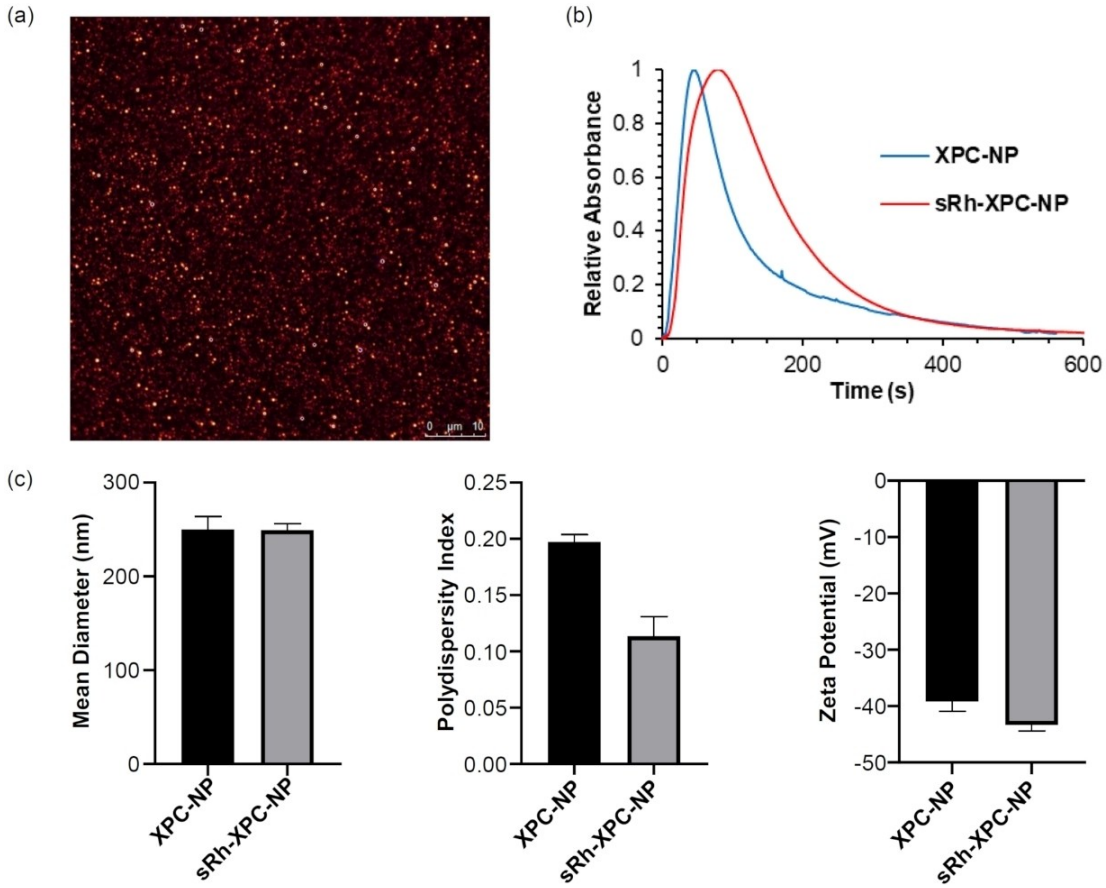

Figure 2. (a) Confocal microscopy images of sulphorhodamine labelled xylan phenyl carbonate nanoparticles (sRh-XPC-NP). Results of (b) disc centrifuge measurements and (c) dynamic light scattering measurements obtained for unmodified XPC-NP and dye-labeled sRh-XPC-NP. Error bars indicate the standard deviation.

dye molecules, was not isolated. Instead, the reaction mixture was directly subjected to dialysis against water in the same way that was used for obtaining unmodified XPC-NP. Colored dispersions of sulforhodamine-labeled XPC-NP (sRh-XPC-NP) were obtained that were characterized by fluorescent confocal laser scanning microscopy, disc centrifuge (CPS) measurements, and dynamic light scattering (DLS; Figure 2). Based on the microscopic images it is clear that the aqueous dispersions of sRh-XPC-NP featured discrete localization of dye molecules on the particles. Previous electron microscopy studies using similar polysaccharide-based NP with physically incorporated dyes and dyes that were covalently fixed to the surface demonstrated defined spherical shapes.[12,14a] The original XPC-NP as well as dye-labeled sRh-XPC-NP prepared by the new *in situ* approach showed very similar particles sizes ($\approx$250 nm), PDI ($\approx$0.1 to 0.2), and zeta potential (≈ -40 mV). CPS experiments demonstrated a monomodal and narrow size distribution, which is important for the later antibody functionalization and application of the particles.[17] PDI values $\leq$0.2 were determined for both particles using DLS. This is consistent with previous results using similar hydrophobic polysaccharide derivatives and indicates that rather uniform NP were formed in both cases.[12] No leaking of the water-soluble dye during dialysis or storage of the colored particle dispersions was observed. This strongly suggests that covalent linkage occurred considering the high efficiency for the conversion of XPC with amines in organic media. Overall, it can be concluded that the new approach for obtaining dye-labeled polysaccharide NP was successful.

Functionalization of Xylan Phenyl Carbonate Nanoparticles with Tumor Targeting Antibodies

Functionalization of XPC-NP with two antibodies was studied; Cetuximab (CTX) as an anti-epidermal growth factor receptor (anti-EGFR) and Atezolizumab (ATZ) as an anti-programmed death-ligand 1 (anti-PD-L1). Both antibodies were conjugated onto the surface of XPC-NP in order to facilitate targeting of tumor cells. Antibody solutions with a predefined amount of 25 to 200 μg of antibody per mg of XPC were added directly to the aqueous particle dispersions. The latter were previously diluted with MES buffer (pH 7). No other coupling- or activation reagents were added, which is a clear advantage over other bio-immobilization strategies that require additional process steps.

After incubation for 24 h at room temperature, excess reagents were removed by consecutive centrifugation and washing and the amount of coupled antibodies was quantified

by determining the amount of uncoupled antibodies in the supernatant of the reaction by UV-Vis spectroscopy (Figure 3). It should be noted that phenol is liberated upon binding of antibodies or other compounds with amino groups to the XPC-NP but the total amount of phenol is too low to be detected by UV-Vis spectroscopy. A coupling efficiency of 100% was observed for immobilization of CTX and ATZ onto XPC-NP when using up to 50 $\mu g_{antibody}/mg_{XPC}$. Further increasing the amount of antibodies still resulted in a further increase in the amount of antibodies bound to the NP surface, however, the coupling efficiency decreased to 43% (CTX) and 57% (ATZ) when reaching 200 $\mu g_{antibody}/mg_{XPC}$. Thus, a certain amount of antibodies was not immobilized meaning that it is important to balance high loading capacity *vs.* increasing costs for antibodies when preparing functionalized XPC-NP for specific drug delivery applications. The functional bioassays demonstrated that the antibodies are indeed fixed to particles surface despite several washing steps. Thus, covalent linkage to the XPC-NP through the formation carbamate bonds can be assumed. It is not possible to directly proof the formation of carbamate bounds on the particle surface, e.g., through spectroscopic methods such as IR or NMR, because the majority of the XPC bulk material remains intact. However, a significant contribution of unspecific binding of antibodies to the hydrophobic XPC-NP is unlikely. Previous work using similar hydrophobic NP derived from cellulose acetate (no reactive groups available) and cellulose acetate phthalate (reactive carboxy groups available) have demonstrated that significant binding of antibodies and dyes under aqueous conditions was only achieved by exploiting covalent coupling strategies but not through non-covalent adsorption.[18] Carbamates bonds are rather stable under the mild conditions used herein (room temperature, neutral pH values, no strong acids/bases).[19] Significant hydrolysis of carbamates requires strongly alkaline conditions and is especially pronounced for aryl carbamates that liberate phenolic compounds. This is not the case for the aliphatic carbamates by conversion of XPC with the amino groups of CTX and ATZ. Moreover, hydrolysis of carbamate groups would be a heterogeneous process at the surface of the XPC, i.e., the reaction rate is further decreased by diffusion of reactants.

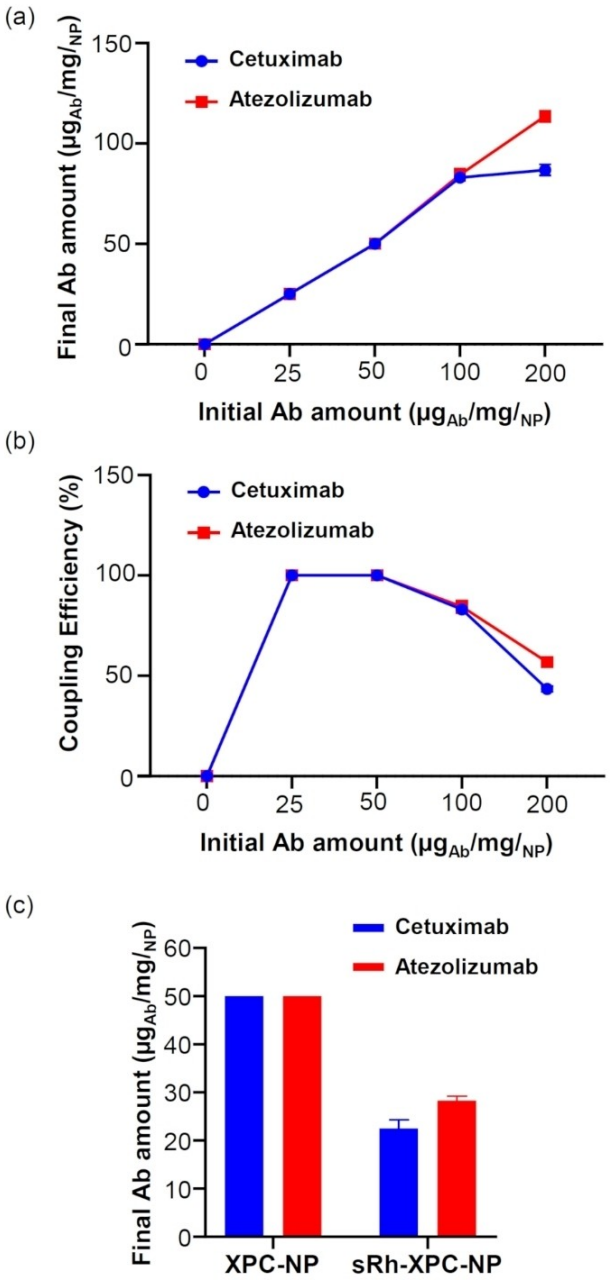

Figure 3. (a) Total amount of coupled antibody (Ab) and (b) coupling efficiency, determined for the immobilization of Cetuximab and Atezolizumab onto xylan phenyl carbonate (XPC) nanoparticles NP (connecting lines were provided to guide the eye). (c) Total amount of coupled Ab for the conversion of XPC-NP and sulphorhodamine-labeled particles (sRH-XPC-NP) using an initial amount of 50 $\mu g_{Ab}/mg_{NP}$. Error bars indicate the standard deviation.

Both antibodies could also be coupled immobilized onto dye modified sRh-XPC-NP. The coupling efficiency determined at 50 $\mu g_{antibody}/mg_{XPC}$ NP (46% for CTX and 56% for ATZ) was found to be lower compared to unmodified XPC-NP (Figure 3c). The decrease in antibody coupling efficiency above a certain concentration threshold is most likely the result of steric hindrance at the particle surface by the bulky antibodies will increase with increasing antibody content making further conversions more difficult. This is supported by DLS and CPS measurements that demonstrate an increase in particle size upon antibody coupling (Figure 4, see Figure S1 in supporting information). The reason for the slightly decreased antibody binding efficiency of sRh-XPC-NP is not clear. A small amount of reactive PC moieties is consumed by dye molecules. Moreover, it can be speculated that the hydrophilic dye preferably accumulates at the surface of the hydrophobic XPC-NP thus shielding the particles.

The particle size was monitored over the different steps of the functionalization of XPC-NP with antibodies including the final conversion with ethanolamine (Figure 4). This last step was performed with an excess of reagent (about 3 equivalents per reactive group in the whole bulk material) to block the remaining reactive XPC moieties and avoid undesired reactions in the biological experiments such as binding of proteins *in vivo*. Previous experiments have demonstrated that this approach does not impact the particle size and shape and

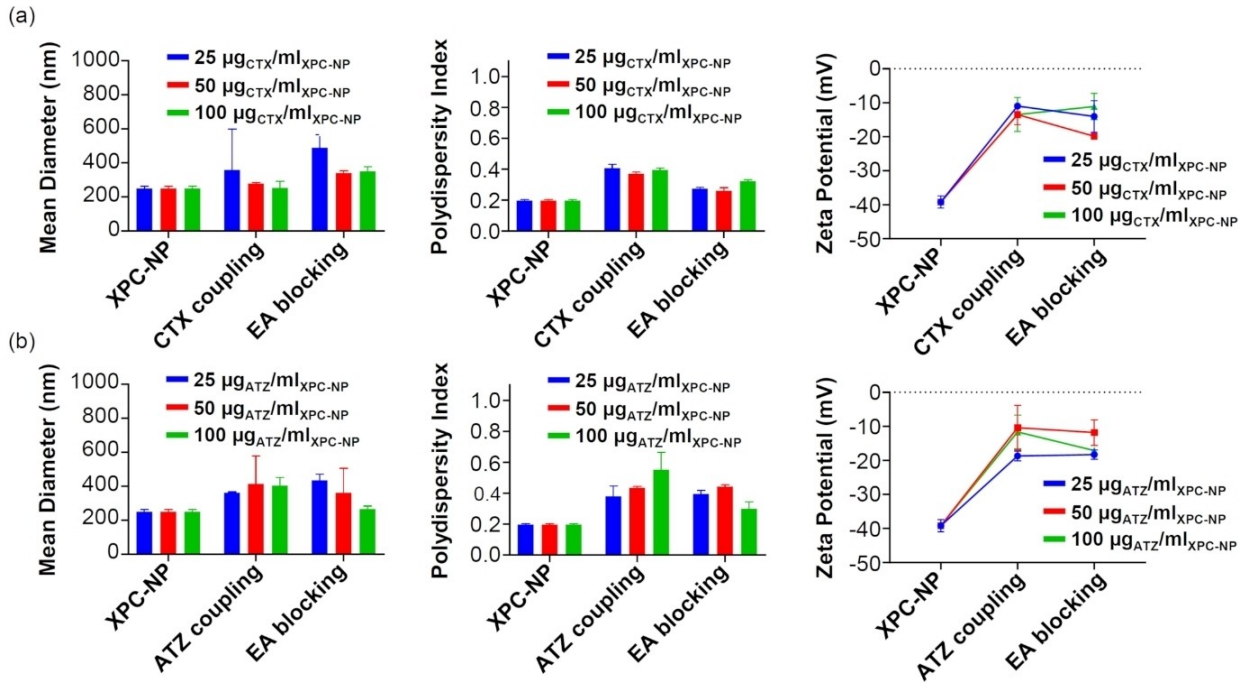

Figure 4. Results of dynamic light scattering measurements obtained for unmodified xylan phenyl carbonate nanoparticles (XPC-NP) and XPC-NP that were functionalized with tumor targeting antibodies (a) Cetuximab (CTX) or (b) Atezolizumab (ATZ) as well as ethanolamine (EA). Error bars indicate the standard deviation and connecting lines were provided to guide the eye.

yields biocompatible NP.[14b] For unmodified XPC-NP, a mean particle diameter of 250 nm was determined by DLS measurements (Figure 4). CPS measurements demonstrated that no agglomeration of the particles into larger aggregates occurred during the procedures used for immobilization of antibodies as indicated by the monomodal distribution (see Figure S1 in supporting information). According to the DLS measurements, particles sizes increased slightly to around 300 to 400 nm. This is reasonable considering that the antibodies are rather large molecules (molecular weight about 145 kg/mol) and attaching these to spherical NP will ultimately increase the diameter of the particles. DLS measurements of the native antibodies showed sizes in the range of 10 to 15 nm and a tendency to form lose aggregates. The absolute value of the zeta potential of XPC-NP −40 mV decreased upon functionalization with antibodies followed by ethanolamine from −40 mV (unmodified particles) to values around −20 to −10 mV. This is the result of the introduction of hydroxyethyl carbamate moieties that are more hydrophilic than aryl carbonates and thus increase the zetapotential. Despite the slight size increase and change in zeta potential, the aqueous particle dispersions of functionalized XPC-NP remained stable and showed no sedimentation over the subsequent experiments.

The coupling experiments were also performed with dye-labeled XPC-NP using 50 µg tumor-targeting antibodies (CTX and ATZ) per ml of particle dispersion. The antibody-labeled particles were characterized and the results were compared with the analogue experiments using none-labeled XPC-NP (Figure 5). No significant differences in terms of particle size, size distribution, and zeta-potential were observed. Thus, sRh-XPC-NP (with and without immobilized antibodies) can be used the later experiments (e.g., incubation with cells followed by confocal microscopy) without expecting that they behave differently compared to XPC-NP without dye labels.

Binding of Antibody-Labeled Xylan Phenyl Carbonate Nanoparticles with Receptor Targets

It was demonstrated that antibodies can be immobilized onto the surface of XPC-NP with high efficiency. However, this could result in blockage of the respective antigen-binding sites by unfavorable binding. Experiments with a quartz crystal microbalance with dissipation monitoring (QCM-D) were performed in order to confirm if the antibody-labeled XPC-NP are able to bind to the respective cell specific target proteins (Figure 6 a). CTX-XPC-NP were employed exemplarily. CTX inhibits the growth of tumors by binding to EGFR that is present in cancer cells.[20] Thus, EGFR was immobilized on the surface of QCM-D sensor chips. When aqueous dispersions of XPC-NP or ATZ-XPC-NP flow through the chamber, no significant change in the oscillation frequencies were observed. This is a clear indication that the XPC-NP bound neither specifically nor unspecifically to the EGFR-modified sensor surface. On the contrary, a significant drop of Δ frequency by about – 30 Hz as well as a strong increase of the dissipation was observed when a flow of CTX-XPC-NP was passed through the device. The changes in oscillation frequency and dissipation clearly indicate the deposition of additional mass, i.e., CTX-XPC-NP, onto the EGFR-modified sensors. This finding proves that CTX-XPC-NP selec-

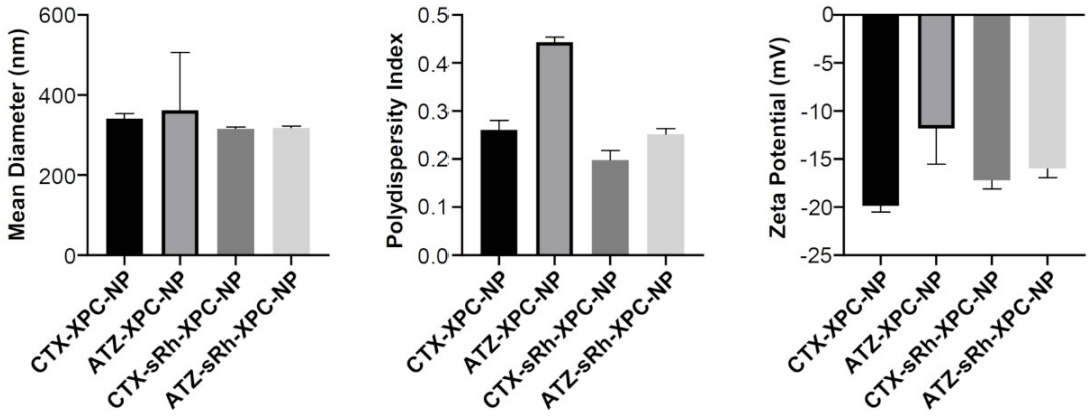

Figure 5. Results dynamic light scattering measurements obtained for xylan phenyl carbonate nanoparticles (XPC-NP) and sulphorhodamine-labeled particles (sRH-XPC-NP) that were coupled with tumor targeting antibodies (CTX: Cetuximab; ATZ: Atezolizumab). Error bars indicate the standard deviation.

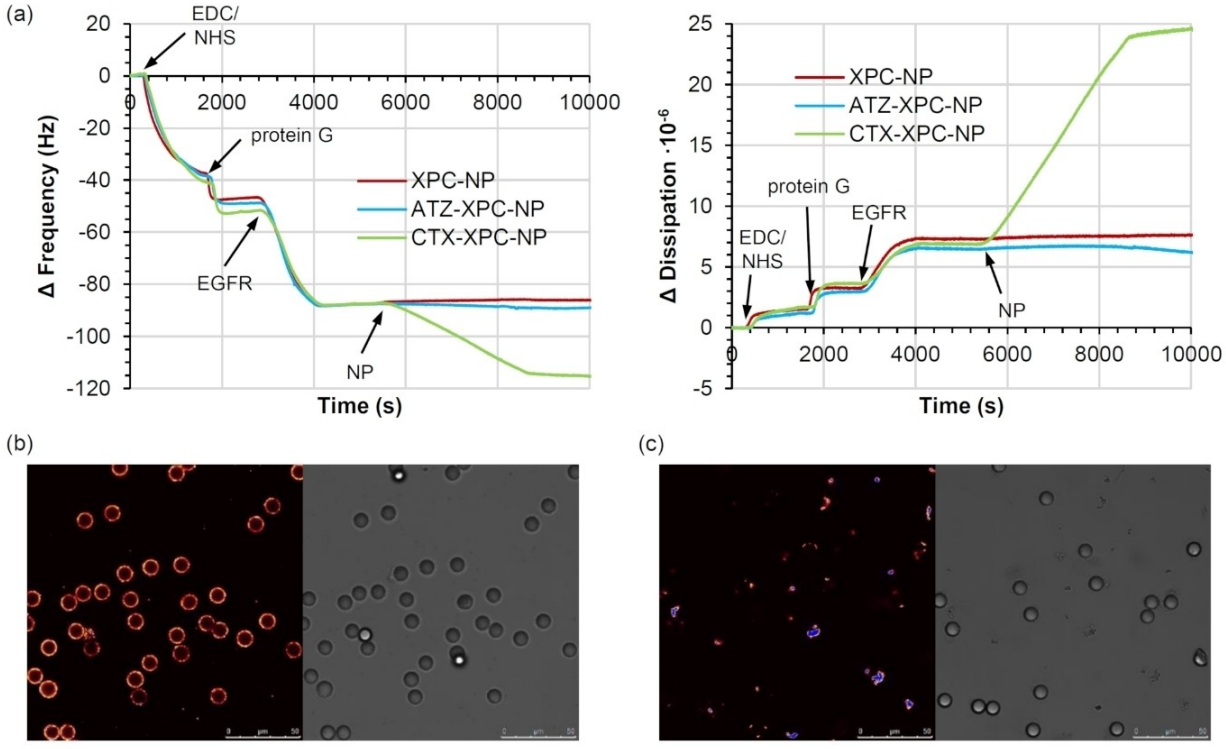

Figure 6. (a) Results of quartz crystal microbalance experiments with dissipation monitoring (QCM-D) using xylan phenyl carbonate nanoparticles (XPC-NP) that partly were functionalized (50 $\mu g_{antibody}/mg_{NP}$) with tumor the targeting antibodies Cetuximab (CTX) or Atezolizumab (ATZ) and finally treated with ethanolamine to block non-specific binding. Before rinsing with aqueous NP dispersions, the CTX-binding epidermal growth factor receptor (EGFR) was fixed to the surface of the QCM-D sensors that were previously modified with protein G by using 1-ethyl-3-(3-dimethylaminopropyl) carbodiimide (EDC) and *N*-hydroxysulfosuccinimide (NHS). (b and c) Confocal microscopy images EGFR-modified polystyrene particles after incubation with of sulphorhodamine nanoparticles (sRh-XPC-NP) that were modified (b) with CTX or (c) with ATZ.

tively bind to EGFR. A similar qualitative behaviour would be expected when using soluble CTX, albeit with a different quantitative change due to the lower mass and size of the antibody compared to CTX-XPC-NP. It should be pointed out in this context that XPC-NP and antibody modified XPC-NP were treated with ethanolamine prior to the bioassays in order to prevent undesired covalent linking, e.g., with EGFR (in the QCM-D experiments) or proteins (in vitro experiments). Moreover, buffer solution was passed through the QCM-D device after each step before switching to the next step.

An additional experiment was conducted to visualize specific binding of CTX-XPC-NP. EGFR was immobilized onto polystyrene microparticles (diameters about 10 μm). After incubation with CTX-sRh-XPC-NP, formation of a corona around the microparticles was observed by confocal laser scanning microscope imaging (Figure 6b), due to binding to EGFR and accumulation of the dye-labeled NP on the microparticle

surface. On the contrary, no corona formation was observed when ATZ-sRh-XPC-NP were used instead. Thus, it can be concluded that the approach for immobilization of antibodies to polysaccharide-based NP presented herein is viable to achieve tumor cell specific targeting and keeps the specific recognition function of the CTX active (Figure 6c).

In Vitro Biological Assays

CTX binds specifically to EGFR. Two cell lines, namely FADU (EGFR positive) and DAUDI (EGFR negative) were chosen to evaluate the specific cellular binding of dye labeled CTX-sRh-XPC-NP by flow cytometry experiments (Figure 7). The cell lines MDA-MB-231 (PD-L1 positive) and THP-1 (PD-L1 negative) were selected to evaluate the cellular binding of ATZ-sRh-XPC-NP. Prior to that, it was confirmed that these cell lines are indeed suitable to study the selective binding by using fluorescence-labeled anti-EGFR and anti-PD-L1 (see Figure S2 in supporting information). Moreover, a comparative analysis of the data was performed (see Figure S3 in supporting information).

For FADU cells, which express EGFR on their surface, a strong binding of CTX-sRh-XPC-NP was observed in the flow cytometry assays. On the contrary, no significant binding was observed for of sRh-XPC-NP that did not carry the EGFR binding CTX. It was also demonstrated that incubating the cells with CTX prior to the treatment with NP effectively blocks the possibility for CTX-XPC-NP to selectively bind to the cell surface. The same experiments were repeated with DAUDI cells. As expected, no significant binding was observed in all cases. Thus, it was proven that (i) CTX-XPC-NP binds to FADU cells and that (ii) this binding is the result of a specific interaction of CTX with EGFR on the surface of the cells. Flow cytometry assays with ATZ-sRh-XPC-NP were performed in an analogue way as described for CTX-sRh-XPC-NP but using cell lines that either do (MDA-MB-231) or do not carry PD-L1 (THP-1). A strong binding was observed only in the case of MDA-MB-231 cells after incubation with ATZ-sRh-XPC-NP. Non-specific binding can be excluded since neither the combination of MDA-MB-231 cells and sRh-XPC-NP (without ATZ) nor THP-1 cells (PD-L1 negative) and ATZ-sRh-XPC-NP resulted in significant binding. The finding that pretreating MDA-MB-231 cells with ATZ inhibited the subsequent binding of ATZ-sRh-XPC-NP proves that the antibody functionalized NP specifically interact with the THP-1 receptor.

EGFR is responsible for the proliferation of cells and blocking the receptor, e.g., by binding of CTX-XPC-NP, would inhibit the cellular growth.[21] Cell viability tests were performed on FADU (EGFR positive) and DAUDI (EGFR negative) cells that were incubated with CTX or CTX-XPC-NP (Figure 8 a and b). The mass concentrations were adjusted in such a way that the amounts of CTX matched the amount of antibody in CTX-XPC-NP, i.e., the total amount of antibodies were the same in both cases (free *vs.* NP-bound). As expected, CTX showed no cytotoxic effect towards DAUDI cells and the same was demonstrated for CTX-XPC-NP. This finding is consisted with previous work that demonstrated that XPC-NP are non-cytotoxic and suitable for biomedical applications.[14b] On the contrary, treating FADU cells with increasing amounts of CTX or CTX-XPC-NP strongly inhibited the cell growth. At mass concentrations of 10 mg_{CTX}/ml, the cell viability decreased to about 40 to 60 %, which can be considered as a strong cytotoxic effect. This mass concentration at which a clear bioactivity occurred was chosen for the flow cytometry and the confocal microscopy imaging experiments. Interestingly, the cytotoxicity was only depended on the total amount of CTX and not by

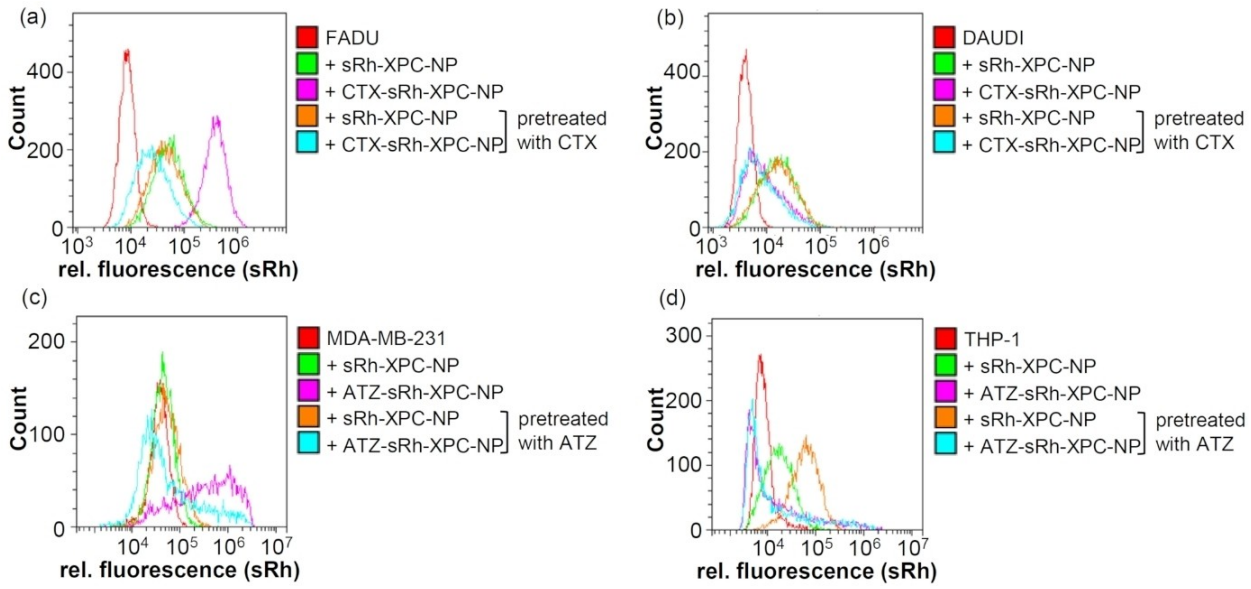

Figure 7. Results of flow cytometry assays carried out with the cell lines (a) FADU (EGFR positive), (b) DAUDI (EGFR negative), (c) MDA-MB-231 (PD-L1 positive), and (d) THP-1 (PD-L1 negative) after incubation with sulphorhodamine (sRh)-labeled xylan phenyl carbonate nanoparticles (XPC-NP) that were functionalized (50 $\mu g_{antibody}/mg_{NP}$) with the tumor targeting antibodies (a and b) Cetuximab (CTX; targets epidermal growth factor receptor/EGFR) or (c and d) Atezolizumab (ATZ; targets programmed death-ligand 1/PD-L1).

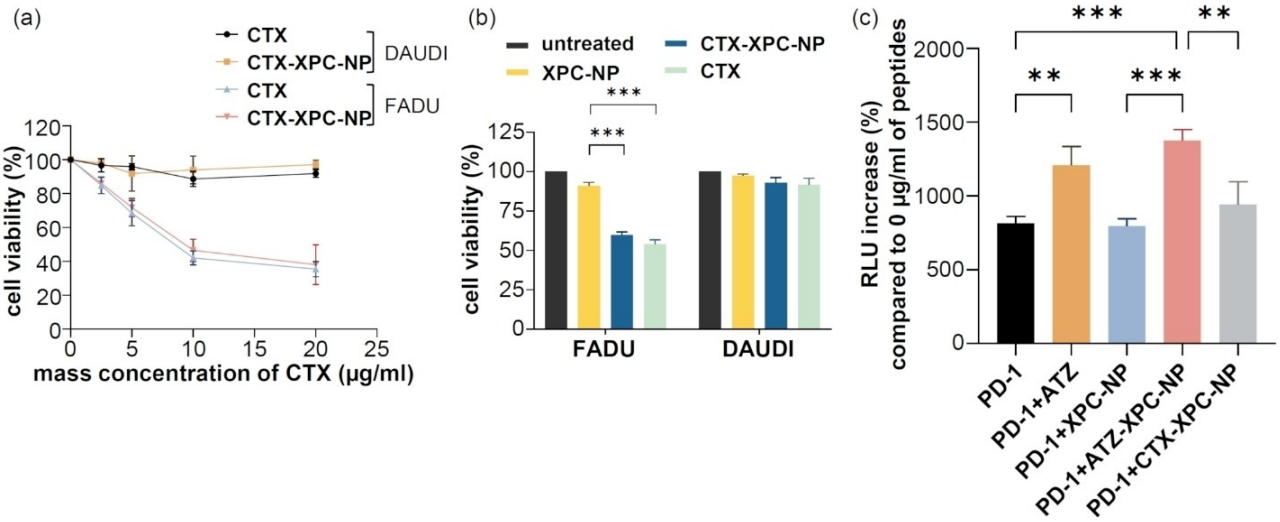

Figure 8. Results of cell assays carried out with sulphorhodamine (sRh)-labeled xylan phenyl carbonate nanoparticles (XPC-NP) that were functionalized (50 $\mu g_{antibody}/mg_{NP}$) with the tumor targeting antibodies Cetuximab (CTX; targets epidermal growth factor receptor/EGFR) or Atezolizumab (ATX; targets programmed death-ligand 1/PD-L1) and different cell lines (FADU: EGFR positive, DAUDI: EGFR negative, MDA-MB-231: PD-L1 positive, Jurkat.PD1-NFAT-Luc). (a and b) Cell viability of FADU and DAUDI cells after incubation with CTX and XPC-NP (with or without CTX). (c) Luciferase activity in Jurkat cells co-cultured with E7 peptide stimulated MDA-MB-231 cells expressed by relative luminescence unit (RLU) increase. Statistical significance was determined by one-way ANOVA followed by a Tukey-Kramer post-hoc test (** $P < 0.01$, *** $P < 0.001$). Error bars indicate the standard deviation.

whether or not CTX was administered as free form or bound to XPC-NP (Figure 8 b). Thus, the activity of CTX was not diminished by the immobilization onto XPC-NP, which demonstrates that these NP can be an efficient delivery system for therapeutic antibodies.

ATZ is a humanized monoclonal antibody that selectively binds to the PD-L1 receptor, blocks PD-1/PD-L1 interaction and by that restores T cell activity within the tumor microenvironment (see Figure S4 in supporting information).[22] In order to evaluate the functional activity of ATZ and ATZ-XPC-NP, a Jurkat.PD1-NFAT-Luc-E7-TCR T cell line was co-cultured with E7 peptide stimulated MDA-MB-231 cells. PD-1/PD-L1 interaction between both cell types inhibited E7-TCR signaling and NFAT-mediated luciferase activity in Jurkat.PD1-NFAT-luc-E7-TCR T cells. The addition of ATZ to the cell culture resulted in a significant increase of luciferase activity, which can be explained by the fact that ATZ binds to the PD-L1 and thus diminishes the inhibitory effect (Figure 8 c). Neither the addition of XPC-NP nor CTX-XPC-NP resulted in a significant increase of luciferase activity. Thus, it can be concluded that no unspecific binding of the PD-L1 receptor with the XPC-NP or antibodies in general occurred. This is a strong indication that immobilization of the antibodies ATZ and CTX onto XPC-NP was also not the result of unspecific binding but rather a covalent fixation through a carbamate bond formation. A significant increase in luciferase activity was observed when the cells were cultivated in the presence of ATZ-XPC-NP. ATZ binds to the corresponding PD-L1 receptor in a specific antibody-antigen interaction. The activity of unbound ATZ and ATZ-XPC-NP was very similar. Thus, it can be concluded again that immobilization of antibodies to reactive XPC-NP is feasible and does not interfere with their ability to bind to the corresponding antigen.

The flow cytometry experiments and biological assays confirmed that the antibody carrying XPC-NP specifically interact with cells carrying the corresponding antigens and can be used as therapeutic agents. Confocal laser scanning microscopy experiments were performed to evaluate the cellular uptake of dye labeled CTX-XPC-NP and ATZ-XPC-NP (Figure 9),

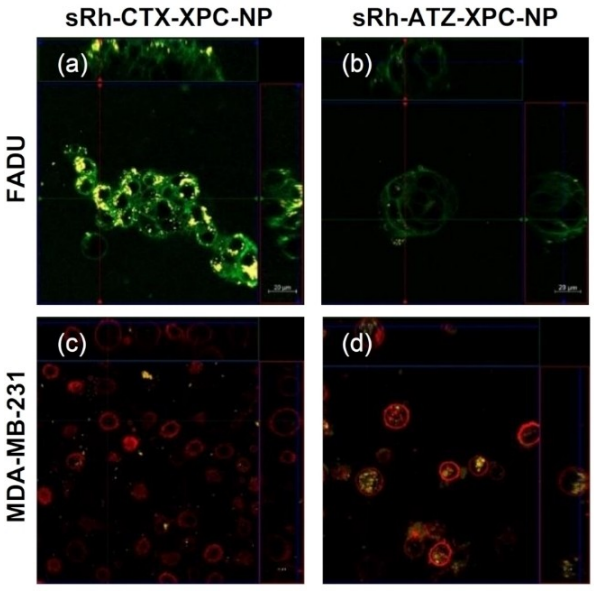

Figure 9. Confocal laser scanning microscopy images of (a and b) FADU cells (EGFR positive/green) and (c–d) MDA-MB-231 cells (PD-L1 positive/red) after incubation with sulphorhodamine (sRh)-labeled xylan phenyl carbonate nanoparticles (XPC-NP/yellow) that were functionalized with the tumor targeting antibodies (a and c) Cetuximab (CTX; targets epidermal growth factor receptor/EGFR) or (b and d) Atezolizumab (ATZ; targets programmed death-ligand 1/PD-L1).

which is a prerequisite for the application as cell specific drug delivery agents. For FADU cells (EGFR positive) a pronounced uptake of CTX-sRh-XPC-NP was observed as indicated by a strong fluorescence within the individual cells after incubation with the particle dispersion. Incubation of FADU cells with NP that did not carry CTX (in this case ATZ-sRh-XPC-NP) resulted in less pronounced fluorescence, i.e., less pronounced cellular uptake. Similar findings were observed for MDA-MB-231 cells (PD-L1 positive) that showed a pronounced uptake of ATZ-sRh-XPC-NP (due to interaction of ATZ with PD-L1) and a less pronounced uptake of CTX-sRh-XPC-NP. Thus, it can be concluded that the cellular uptake of CTX- and ATZ-functionalized XPC-NP within tumor cells is the result of interactions of the antibodies with tumor specific antigens. Additional proof for the cellular uptake can be gained from 3D-images that showcase the localization of cells and the dye-functionalized XPC-NP within (see Supporting Information).

Conclusions

Two types of tumor targeting antibodies, namely Cetuximab (CTX; targets epidermal growth factor receptor/EGFR) and Atezolizumab (ATZ; targets programmed death-ligand 1/PD-L1), were successfully immobilized to reactive xylan phenyl carbonate nanoparticles (XPC-NP). High coupling efficiencies of up to 100% were achieved in this one-step process and no aggregation of the NP was observed. It was demonstrated that the specific bioactive role of CTX and ATZ was retained during the coupling process and that the functionalized NP obtained this way interact with cell through specific antibody-antigen interaction. This work presents a facile approach to obtain antibody functionalized polysaccharide NP that can be tailored to target specific cell types such as cancer cells. These materials possess great potential for therapeutic purposes. In summary, this innovative approach of developing tumor-targeting antigen-selective polysaccharide NP holds great promise for personalized and effective cancer therapy, offering enhanced selectivity, prolonged drug release, and potential synergistic effects with other therapeutic modalities. Future studies based on these results will focus on *in vitro* cell targeting and localization of antibody-labeled XPC-NP as well as on cell specific drug delivery and release.

Experimental Section

Materials

N,*N*-dimethyl acetamide (DMA), triethylamine, poly(sodium-4-styrenesulfonate) (PSS; molecular weight 70 000 g/mol), 1-ethyl-3-(3-dimethylaminopropyl) carbodiimide (EDC), buffer solution salts, Tween 20, sodium thioglycolate, and 2-(*N*-morpholino) ethanesulfonic acid (MES) were obtained from Sigma-Aldrich. Dialysis membrane Spectra/Por® 3; molecular weight cutoff 3 500 g/mol; 18 mm Flat Width was purchased from Spectrum Laboratories. Poly(allylamine hydrochloride) (PAH; molecular weight 40 000 g/mol) was purchased from Beckmann-Kenko in Bassum, Germany, and *N*-hydroxysulfosuccinimide (NHS) was acquired from Fluorochem in Hadfield, UK. Xylan phenyl carbonate (XPC) with a degree of substitution of 1.94 (which describes to amount of functional groups per repeating unit) was prepared according to the literature.[14a] Sulforhodamine (sRh) amine for labelling of XPC nanoparticles (NP) was synthesized as described before.[23] Polystyrene-based spherical microparticles were manufactured by Surflay Nanotec GmbH.

Streptococcal protein G with only Fc-binding capabilities and Fc-fusion human epidermal growth factor receptor (EGFR-Fc) were purchased from Sigma-Aldrich and R&D Systems Inc. in Minneapolis, MN, respectively. HPV16-$E7_{11\text{-}20}$ ($E7_{11\text{-}20}$) peptide was purchased from Peptides & Elephants (Berlin, Germany). Anti-human PD-L1 (clone MIH3) was purchased from BioLegend, and anti-human EGFR (clone h, SC120-FITC) was from Santa Cruz, United States. Anti ERBB2 antibody (clone 24D2, FITC) and anti HLA-A2 antibody (clone BB7.2, APC) were purchased from Biolegend (San Diego, United States). Tumor targeting antibodies Cetuximab (CTX) and Atezolizumab (ATZ) used for functionalization of XPC-NP were obtained from University Medical Center Groningen (UMCG) hospital pharmacy. The CellTiter 96® AQueous Non-Radioactive Cell Proliferation Assay kit, and Luciferase Assay Reagent Bio-Glo were obtained from Promega (Madison, USA).

FADU, DAUDI, MDA-MB-231, THP-1, Jurkat.PD1-NFAT-luc T cells, and Jurkat-NFAT-luc T cells were obtained from American Type Culture Collection. Cell lines were cultured either in Roswell Park Memorial Institute (RPMI) medium or Dulbecco's Modified Eagle's medium (DMEM; Lonza, Biowhittaker BE12-604F and BE12-155F) supplemented with 10% fetal calf serum (FCS; Gibco™ Fetal Bovine Serum, USA) at 37 °C in a humidified 5% CO_2 atmosphere and underwent routine PCR testing for excluding mycoplasma infections.

Methods

The particle size, zeta potential, and polydispersity index (PDI) of XPC-NP as well as antibody and/or dye functionalized XPC-NP were evaluated using MalvernZetasizer Nano ZSP (Malvern Panalytical Ltd. UK). Aqueous particle suspensions were diluted with TRIS buffer (pH value of 7) volume ratio: 1:100) before being subjected to the experiments. A disc centrifuge (CPS) from DC Instruments, Inc., USA was used to evaluate the particle size distribution and most notably if the distribution was monomodal. Determination of antibody coupling efficiency was done by utilizing a UV-VIS spectrophotometer (Cary 50, Agilent, United States) and assessing the absorbance of the antibody at 280 nm wavelength.

A quartz crystal microbalance device with dissipation monitoring (QCM-D; QSense analyzer, Biolin Scientific, Sweden) was utilized to monitor the interaction of antibody functionalized. Prior to the experiments, the QCM-D gold surface of the sensors were incubated with thioglycolic acid (1 mM) at 25 °C overnight to generate carboxy groups on the surface. The experiments were started by pumping buffer (pH value of 6.4) through the system followed by solutions of (i) EDC/NHS (0.2 M each), (ii) protein G (0.2 mg/ml), (iii) EGFR (20 μg/ml) and finally (iv) aqueous NP dispersions (1 mg/ml). After each individual step, buffer was pumped through the system for some time before switching to the next step. All NP used in the QCM-D experiments were treated with ethanolamine as described above to prevent undesired covalent linking with EGFR.

UV-VIS spectrophotometer (Cary 50, Agilent, United States) was utilized to determine antibody coupling efficiency by assessing the absorbance of the antibody at 280 nm wavelength. This was accomplished by measuring the antibody concentration in the

supernatant after coupling. Confocal laser scanning microscope images of cells were recorded on a Zeiss cell discoverer 7 microscope equipped with a PlanApochromat 50×/1.2 water (WD = 0.84 mm) objective attached to a 0.5× optovar lens and a LSM900 confocal head (Germany, Jena). Diode lasers with wavelength of 488 nm (excitation of fluorescein/Fl) and 561 nm (excitation of sulforhodamine/sRh and allophycocyanin/APC) were employed together with an Airscan 2 detector. All images were processed with ZEN blue (V3.5) software. A confocal laser scanning microscope (Leica TCS SPE, TYPE DMI4000 CS, Germany) was utilized to evaluate the XPC-NP morphology and their ability to bind to antibody modified surfaces. For the latter experiments, polystyrene particles (9.44 ± 0.017 μm, containing a coumarin dye) were coated with PAH and PSS using a layer-by-layer self-assembly technique.[24] Subsequently, the particles were treated with aqueous EDC/NHC (0.2 M each), followed by solutions of protein G (0.2 mg/ml), and finally EGFR (20 μg/ml). sRh labeled CTX-XPC-NP and ATZ-XPC-NP were incubated with freshly prepared EGFR coupled polystyrene sensor particles for 30 min at 25 °C and the samples were observed under a confocal scanning laser microscope.

Preparation of Nanoparticles

The XPC-NP dispersions were prepared according to literature (figure 1).[18b] A defined amount of XPC (50 mg) was dissolved in DMA (11 ml) under magnetic stirring for 30 minutes. The solution was centrifuged (10 min, 9800 g) to remove dust particles. The optically clear solution was dialyzed (regenerated cellulose membrane, 3.5KD molecular weight cut-off) against 1 L of deionized water. The water was renewed five times over the course of two days.

In order to label XPC-NP with sRh, XPC (50 mg) was dissolved in DMA (11 ml) solution under magnetic stirring for 30 min in a round bottom flask. sRh amine (0.8 mg; 0.01 mol dye per mol of reactive phenyl carbonate moieties) together with triethylamine (0.4 mg) were dissolved in DMA for 30 min. Both solutions were combined and stirred at 60 °C for 4 h. After cooling to room temperature, the solution was centrifuged and subjected to NP preparation by dialysis as described above.

Functionalization of XPC-NP with antibodies was performed by direct immobilization without preactivation (Figure 1). The experiments were performed using particle dispersions with a starting mass concentration of 1 mg/ml. The aqueous XPC-NP dispersions (1 ml, 1 mg/ml) were centrifuged (10 min, 9800 g) to remove water and XPC-NP were dispersed in MES buffer (50 mM, pH value of 7) containing different amounts of antibodies and the dispersion was incubated on a rotary shaker for 24 h at 25 °C. The total volume (buffer and antibody stock solution) was adjusted to 1 ml and the final mass concentration of antibodies was adjusted to be between 25 μg/ml and 300 μg/ml. Afterwards, a diluted aqueous solution of ethanolamine (1 ml; 1 M, pH value of 8.5) was added and after 24 h incubation on a rotary shaker at RT the mixture was purified 3-times by centrifugation (10 min, 9800 g), removal of the supernatant, and redispersion in TRIS buffer (1 ml, pH 7.4). The coupling efficiency was determined by determination of the antibody concentration in the first supernatant by UV-Vis spectroscopy at 280 nm. It should be noted that although phenol shows high absorbance at the same wavelength but the concentration is below the detection limit due to the fact that only few phenol molecules are released upon binding of the large antibody molecules. This, no interference with the quantification is expected.

Lentiviral Transduction

A specific TCR towards the human papillomavirus 16 (HPV16) $E7_{11-20}$ peptide (E7-TCR), previously described, was cloned into the pRRL-SFFV-iGFP plasmid (pRRL-SFFV-E7-TCR-iGFP; synthesized by Genscript, Nanjing, China).[25] Human embryonic kidney 293T cells (HEK293T) cells were cultured in DMEM (+10% FCS) in T75 flasks. Lentiviruses containing a pRRL-SFFV-E7-TCR-iGFP plasmid, or as a control an empty pRRL-SFFV-iGFP vector were generated by transient transfection of HEK293T cells using the Fugene transfection system (Promega, Madison, USA), together with packaging construct psPAX2 (Addgene, #12260) and Glycoprotein envelope plasmid pMD2.G (Addgene, #12259). Viral supernatant was harvested and filtered through a 0.45 μm filter after 2 days of the transfection. The virus was concentrated by ultracentrifugation and either used to transduce Jurkat-NFAT-luc T cells or Jurkat.PD1-NFAT-luc T cells (with 8 μg/mL polybrene to increase the infection efficiency) or stored at −80 °C. To assess transduction efficiency, green fluorescent protein (GFP) expression was checked using flow cytometry. Stably transduced cells were sorted for expression of the GFP by fluorescence-activated cell sorting with a Sony cell sorter sh800s.

Flow cytometry Experiments

All experiments were performed in three replicates. Approximately 5×10^4 cells were collected and prepared as a single-cell suspension. For staining, 1 μg of fluorescently labeled antibodies targeting the markers of interest was added to each sample for 30 min at 4 °C. Control samples were included, consisting of unstained cells, cells stained with isotype controls, and cells stained with appropriate positive and negative controls. For NP binding assessment, 5×10^4 cells were treated with XPC-NP at 100 μg/mL (sulforhodamine labeled) for 1 h at 4 °C. The samples were washed twice with phosphate-buffered saline (PBS) and then analyzed using a flow cytometer (CytoFLEX, Beckman Coulter, Fullerton, CA, USA), with a flow rate of 1 μL cells per second. A total of 10,000 events were acquired for each sample. The acquired data were analyzed using flow cytometry analysis software (Beckman Coulter), applying appropriate gating strategies to identify specific cell populations based on their fluorescence characteristics. The results were presented using histograms to visualize the fluorescence intensity.

Assessment of Cell Viability

Cell viability was measured using (3-(4,5-dimethylthiazol-2-yl)-5-(3-carboxymethoxyphenyl)-2-(4-sulfophenyl)-2H-tetrazolium) (MTS) and phenazine methosulfate (PMS) according to manufacturer's protocol (CellTiter 96® AQueous Non-Radioactive Cell Proliferation Assay, Promega). In brief, 1×10^4 cells were suspended in 100 μl of culture medium and seeded into 96-well plates (Costar, Cambridge, MA) for a 24 hour incubation period. Subsequently, various concentrations (2.5, 5, 10, or 20 μg/mL) of CTX or CTX-NP (50, 100, 200, or 400 μg/mL) were added to each well, and the cells were treated for 72 hours. Afterward, 20 μl of 20% (v/v) MTS + PMS solution was added to each well, and absorbance was measured at 490 nM after 1–2 hours of incubation at 37 °C and 5% CO_2. Cells treated with 20 μl of 70% ethanol were included as a background control whereby the obtained absorbance was subtracted from all experimental conditions.

Bioassay for PD-1/PD-L1 Blockade

MDA-MB-231 cells expressing high PD-L1 were seeded at a density of approximately 1×10^4 cells in 100 μl of culture medium into 96-

well plates (Costar, Cambridge, MA) and incubated for 24 hours. The cells were stimulated with HPV-16 E7 peptides (10 μg/mL) for 2 hours. To evaluate PD-1/PD-L1 interaction, Jurkat-NFAT-luc-E7-TCR T cells (expressing E7-TCR and NFAT-inducible luciferase) or Jurkat.PD-1-NFAT-luc-E7-TCR T cells (expressing E7-TCR, PD-1, and NFAT-inducible luciferase) were co-cultured with pulsed MDA-MB-231 cells. Prior to adding the corresponding Jurkat cells at a ratio of 10:1 (effector cells to target cells), the cells were treated with 5 μg/mL of ATZ or 100 μg/mL of ATZ-NP for 15 minutes. After a 6 hour co-culture, 100 μl of the culture medium containing Jurkat cells was collected and transferred to opaque white plates (Costar, Badhoevedorp, The Netherlands). Subsequently, 30 μl of Luciferase Assay Reagent Bio-Glo (Promega) was added to each well, followed by a 15 minute incubation period. Luminescence was measured using a luminometer (Synergy, BioTek, Winooski, VT, USA), and the luciferase activity in Jurkat cells co-cultured with E7 peptide-pulsed MDA-MB-231 cells was expressed as relative luminescence units (RLUs) compared to Jurkat cells co-cultured with non-stimulated MDA-MB-231 cells.

Confocal Microscopy Experiments on Cells

FADU and MDA-MB-231 cells (3×10^4 cells suspended in 300 μL of DMEM containing 10% FCS) were plated in the 8-well borosilicate slides (Nunc Lab-Tek II Chambered coverglass, 154461, ThermoFisher Scientific, United States, Waltham) and incubated overnight at 37 °C with 5% CO_2. Afterwards, dispersions of CTX-sRh-XPC-NP or CTX-sRh-NP (30 μl, 1 mg/ml) and the cells were incubated overnight. After washing with full medium for three times, FADU cells were stained with anti ERBB2 antibody (clone 24D2, FITC) and MDA-MB-231 cells were stained with anti HLA-A2 antibody (clone BB7.2, APC) for 15 min. Confocal microscopy images ware taken at 37 °C with 5% CO_2.

Statistical Analysis

Each measurement was carried out in three separate replicates in quick succession, and the results are shown as the mean values accompanied by the standard deviation as error bars. The P values were generated by analyzing data with two-tailed unpaired t-test using Prism 8 (GraphPad software). Results with $p < 0.05$ were considered to be significant.

Supporting Information

Supporting Information is available from the Wiley Online Library or from the author. The file contains (i) results of centrifuge experiments with all xylan phenyl carbonate nanoparticles (XPC-NP) used in this study, (ii) flow cytometry data that confirm the suitability of all cell lines for evaluation of antigen specific binding, and (iii) schematic representations of the strategy employed for binding of antibody XPC-NP to the programmed death-ligand 1 in T-cells as well as for the Jurkat. PD1-NFAT luciferase E7 TCR model used in this study. In addition, videos were attached that showcase the 3D confocal laser scanning microscopy images of FADU cells and MDA-MB-231 cells after incubation with CTX-sRh-XPC-NP and ATZ-sRh-XPC-NP.

Acknowledgements

V. B. performed experimental work, data curation, and formal analysis related to the preparation, functionalization, and characterization of nanoparticles (NP) including QCM-D experiments. Y. L. performed experimental work, data curation, and formal analysis related to cell cultivation and bioassays including confocal laser scanning microscopy assays. V. B. together with M. G., L. D., and E. B were primarily responsible for the concept of this work. G. H., T. H., E. B., W. W., and G. E. assisted in the conventionalization of the work and the investigation. V. B. and M. G. were responsible for interpretation of the data and wrote the manuscript. Open Access funding enabled and organized by Projekt DEAL.

Conflict of Interests

The authors declare no conflict of interest.

Data Availability Statement

The data that support the findings of this study are available from the corresponding author upon reasonable request.

Keywords: polysaccharide-based nanoparticles · xylan phenyl carbonate · antibody functionalization · tumor-targeting · cetuximab · atezolizumab

[1] S. Gavas, S. Quazi, T. M. Karpiński, *Nanoscale Res. Lett.* **2021**, *16*, 173.
[2] a) I. Jovčevska, S. Muyldermans, *BioDrugs* **2020**, *34*, 11; b) L. C. Sandin, F. Eriksson, P. Ellmark, A. S. Loskog, T. H. Totterman, S. M. Mangsbo, *Oncoimmunology* **2014**, *3*, e27614.
[3] L. Zitvogel, L. Apetoh, F. Ghiringhelli, G. Kroemer, *Nat. Rev. Immunol.* **2008**, *8*, 59.
[4] a) S. Oliveira, R. Heukers, J. Sornkom, R. J. Kok, P. M. van Bergen En Henegouwen, *J. Controlled Release* **2013**, *172*, 607; b) H. Revets, P. De Baetselier, S. Muyldermans, *Expert Opin. Biol. Ther.* **2005**, *5*, 111; c) I. Van Audenhove, J. Gettemans, *EBioMedicine* **2016**, *8*, 40.
[5] a) B. Han, Y. Yang, J. Chen, H. Tang, Y. Sun, Z. Zhang, Z. Wang, Y. Li, Y. Li, X. Luan, Q. Li, Z. Ren, X. Zhou, D. Cong, Z. Liu, Q. Meng, F. Sun, J. Pei, *Int. J. Nanomed.* **2020**, *15*, 553; b) R. K. Jain, *Sci. Am.* **1994**, *271*, 58; c) F. Mottaghitalab, M. Farokhi, Y. Fatahi, F. Atyabi, R. Dinarvand, *J. Controlled Release* **2019**, *295*, 250; d) H. Wang, F. Zhang, H. Wen, W. Shi, Q. Huang, Y. Huang, J. Xie, P. Li, J. Chen, L. Qin, Y. Zhou, *J. Nanobiotechnol.* **2020**, *18*, 8;e) Y. Yao, Y. Zhou, L. Liu, Y. Xu, Q. Chen, Y. Wang, S. Wu, Y. Deng, J. Zhang, A. Shao, *Front. Mol. Biosci.* **2020**, *7*, 193.
[6] C. He, J. Lu, W. Lin, *J. Controlled Release* **2015**, *219*, 224.
[7] a) A. M. Master, A. Sen Gupta, *Nanomedicine (Lond.)* **2012**, *7*, 1895; b) A. Adhikari, V. K. Bhutani, S. Mondal, M. Das, S. Darbar, R. Ghosh, N. Polley, A. K. Das, S. S. Bhattacharya, D. Pal, A. K. Mallick, S. K. Pal, *Pediatr. Res.* **2022**, *93*, 827.
[8] a) A. Behera, D. Rai, S. S. Kulkarni, *J. Am. Chem. Soc.* **2020**, *142*, 456; b) Y. Yu, M. Shen, Q. Song, J. Xie, *Carbohydr. Polym.* **2018**, *183*, 91.
[9] a) X. Liu, J. Xie, S. Jia, L. Huang, Z. Wang, C. Li, M. Xie, *Int. J. Biol. Macromol.* **2017**, *98*, 576; b) Y. Zeng, Y. Xiang, R. Sheng, H. Tomas, J. Rodrigues, Z. Gu, H. Zhang, Q. Gong, K. Luo, *Bioact. Mater.* **2021**, *6*, 3358.
[10] I. A. Schepetkin, M. T. Quinn, *Int. Immunopharmacol.* **2006**, *6*, 317.
[11] a) L. Bugnicourt, C. Ladavière, *Progr. Polym. Sci.* **2016**, *60*, 1; b) M. Yanat, K. Schroën, *Carbohydr. Polym.* **2023**, *312*, 120789; c) H. Yuan, C. Guo, L. Liu, L. Zhao, Y. Zhang, T. Yin, H. He, J. Gou, B. Pan, X. Tang, *Carbohydr. Polym.* **2023**, *312*, 120838.

[12] M. Gericke, P. Schulze, T. Heinze, *Macromol. Biosci.* **2020**, *20*, 1900415.
[13] a) H. Lindemann, M. Kühne, C. Grune, P. Warncke, S. Hofmann, A. Koschella, M. Godmann, D. Fischer, T. Heinzel, T. Heinze, *Macromol. Biosci.* **2020**, 200039; b) M. Kühne, H. Lindemann, C. Grune, D. Schröder, Z. Cseresnyés, M. Godmann, A. Koschella, M. T. Figge, C. Eggeling, D. Fischer, T. Heinze, T. Heinzel, *J. Controlled Release* **2021**, *329*, 717.
[14] a) M. Gericke, L. Gabriel, K. Geitel, S. Benndorf, P. Trivedi, P. Fardim, T. Heinze, *Carbohydr. Polym.* **2018**, *193*, 45; b) M. Gericke, K. Geitel, C. Jörke, J. H. Clement, T. Heinze, *Molecules* **2021**, *26*, 4026.
[15] A. Verma, F. Stellacci, *Small* **2010**, *6*, 12.
[16] L. Gabriel, M. Gericke, T. Heinze, *Carbohydr. Polym.* **2019**, *207*, 782.
[17] S. Clarke, *PhD Thesis Development of hierarchical magnetic nanocomposite materials for biomedical applications*, Dublin City University, **2013**.
[18] a) P. Schulze, M. Gericke, F. Scholz, H. Wondraczek, P. Miethe, T. Heinze, *Macromol. Chem. Phys.* **2016**, 11; b) P. Schulze, M. Gericke, T. Heinze, *Cellulose* **2019**, *26*, 475.
[19] a) P. Adams, F. A. Baron, *Chem. Rev.* **1965**, *65*, 567; b) L. W. Dittert, T. Higuchi, *J. Pharm. Sci.* **1963**, *52*, 852.
[20] S.-F. Wong, *Clin. Ther.* **2005**, *27*, 684.
[21] P. Wee, Z. Wang, *Cancers* **2017**, *9*, 52.
[22] R. Deng, D. Bumbaca, C. V. Pastuskovas, C. A. Boswell, D. West, K. J. Cowan, H. Chiu, J. Mcbride, C. Johnson, Y. Xin, H. Koeppen, M. Leabman, S. Iyer, *mAbs* **2016**, *8*, 593.
[23] M. Beija, C. A. M. Afonso, J. M. G. Martinho, *Chem. Soc. Rev.* **2009**, *38*, 2410.
[24] C. S. Peyratout, L. Dähne, *Angew. Chem. Int. Ed.* **2004**, *43*, 3762.
[25] B. Y. Jin, T. E. Campbell, L. M. Draper, S. Stevanovic, B. Weissbrich, Z. Yu, N. P. Restifo, S. A. Rosenberg, C. L. Trimble, C. S. Hinrichs, *JCI Insight* **2018**, *3*, e99488.

Manuscript received: December 8, 2023
Revised manuscript received: January 11, 2024
Accepted manuscript online: January 18, 2024
Version of record online: February 14, 2024